ELEKTROTEHNIŠKI VESTNIK 88(5): 247-254, 2021
ORIGINAL SCIENTIFIC PAPER

Anti-Saturation PID Control to Improve the Current Response Speed of the Permanent Magnet Spherical Actuator

Rui Zhang [1,2], Guoli Li [1,2,3], Qunjing Wang [1,3,4], Xiuqin Wang[1,2,4], and Yan Wen [2,5]

[1] *School of Electrical Engineering and Automation, Anhui University, Hefei, Anhui, China*
[2] *National Engineering Laboratory of Energy-Saving Motor & Control Technology, Anhui University, Anhui, China*
[3] *Anhui Key Laboratory of Industrial Energy-Saving and Safety, Anhui University, Hefei, Anhui, China*
[4] *Anhui Collaborative Innovation Centre of Industrial Energy-Saving and Power Quality Control, Anhui University, China*
[5] *School of Internet, Anhui University, Hefei, Anhui, China*
E-mail: wangxiuqin@ahu.edu.cn

Abstract. In order to improve the dynamic current response speed of the permanent-magnet spherical actuator (PMSA) in a multi-degree-of-freedom motion, an anti-saturation proportional-integral-derivative (PID) current-controller design method is proposed. In the view of the slow response of the PMSA stator coil current caused by the traditional PID current controller, an anti-saturation link is added according to the controller input and output status. When the input is changed slowly, the function of the integrator is fully utilized to reduce the overshoot. When the input is changed quickly, the integrator exits saturation faster, and the system response speed is improved. The experimental results show that the method controls the stator coil current more accurately than the traditional PID controller, and improves the PMSA current response speed. Two current controllers are used to compare the PMSA motion control. The results show that the proposed control method improves the PMSA dynamic current response performance.

Keywords: Permanent Magnet Spherical Actuator (PMSA); Closed-Loop Current Control; Anti-Saturation; Response Speed

Izboljšanje tokovne odzivnosti sferičnega aktuatorja s trajnim magnetom s krmilnikom proti nasičenju

V prispevku je predstavljen tokovni krmilnik za izboljšanje dinamične tokovne odzivnosti sferičnega aktuatorja s trajnimi magneti. Glede na počasen odziv toka tuljave statorja, ki ga povzroča tradicionalni tokovni krmilnik, je dodana povezava proti nasičenju z upoštevanjem vhoda in izhoda krmilnika. Ko se vhod spreminja počasi, se integrator v tokovnem krmilniku uporabi v celoti za zmanjšanje prekoračitve. Ko se vhod spremeni hitro, aktuator hitreje izstopi iz stanja nasičenja in hitrost odziva se izboljša. Eksperimentalni rezultati kažejo, da metoda natančneje nadzoruje tok statorske tuljave v primerjavi s klasičnim krmilnikom PID in izboljša odzivnost.

1 INTRODUCTION

The manufacturing industry is the main body of the national economy. With the advent of intelligent manufacturing, the demand for industrial robots and other multi-degree-of-freedom (DOF) devices in industrial applications has increased sharply [1-3]. Compared with the traditional single-axis motor, the spherical actuator has a good dynamic performance, realizes a multi-DOF movement on a single motor, has a compact structure, saves a lot of mechanical transmission devices, and improves the overall transmission efficiency of the system. Therefore, it has attracted a wide attention of both the academic sphere and industry [4-6].

In order to enable PMSA to achieve a multi-DOF motion, such as spin and tilt, it is essential to energize the stator coils [7]. In the PMSA motion control system, the stator coil current control generally adopts the traditional proportional-integral-derivative (PID) control. However, when the drive current changes significantly, the integrator will have a large accumulation in the error due to the large change. The PID controller will take more time to adjust the output to reach a steady state, and the dynamic response speed of the drive current will be affected, resulting in a slow response to the step current [8]. This phenomenon that the system response slows down due to the integral link of the PID controller is called integral saturation [9-10]. If the integration link of the traditional PID controller is not corrected, the integral saturation will greatly reduce the dynamic response speed of the driving current, and even destabilize the control system.

Scholars worldwide have conducted research on the integral-saturation phenomenon in control systems, and have mainly proposed two types of anti-integral saturation control algorithms, conditional integral method and inverse calculation tracking method [11-14]. The former chooses to use the integral function according to whether the system output has a limiting function. When the controller is saturated, the integrator function

Received 20 July 2021
Accepted 9 September 2021

is cancelled. The latter is to eliminate the error caused by the integral saturation through the feedback difference calculation, and then to suppress the integral saturation phenomenon. This method is simple in structure, easy to design, and more suitable for practical engineering applications. The paper proposes an anti-integral saturation PID current controller for PMSA. The method adjusts the controller integration state according to the setting value of the stator coil current. When the current setting value is small or the input changes slowly, the integrator fully plays its role by reducing the overshoot. When the current setting value is large or the input changes quickly, the integrator will withdraw from the function and improve the current response speed. The method can greatly improve the PMSA operating performance and maintain a good dynamic response.

The rest of the paper is organized as follows. Section 2 introduces the basic structure and drive model of PMSA. Section 3 presents the traditional PID current controller and the design of the proposed anti-saturation PID current controller. In Section 4, an experiment is conducted with a single anti-saturation PID current controller and a PMSA motion comparison experiment is made. Section 5 concludes the paper.

2 PMSA STRUCTURE AND DRIVE MODEL

2.1 PMSA mechanical structure

The proposed PMSA is mainly composed of a spherical rotor, a stator composed of two hemispherical shells and an output shaft fixed on the rotor [15-16]. The overall PMSA structure is shown in Figure 1(a), and the rotor and stator coils in Figure 1(b). Four layers of 40 permanent magnets (PMs) are symmetrically and evenly distributed on both sides of the rotor equator, with an alternating N and S poles arrangement, and the angle between the columns is 36°. There are two layers of the stator coils symmetrically distributed along the equator on the stator shell, and each layer contains 12 coils at equal intervals, and the angle between the columns is 30°. The PMSA major specification is shown in Table 1. The current flowing through the stator coil generates an electromagnetic field, which interacts with PMs to generate an electromagnetic torque to drive the rotor. Affected by the mechanical structure, the PMSA tilt motion range is 0-37.5° and the spin range is 0-360°.

Table 1. PMSA major specification

Parameter	Value
Radius of rotor(mm)	64
Inner radius of coil(mm)	4
Outer radius of coil(mm)	14
Height of coil(mm)	25
NI(A)	2400
Radius of PM(mm)	10
Height of PM(mm)	12
Length of air gap(mm)	1

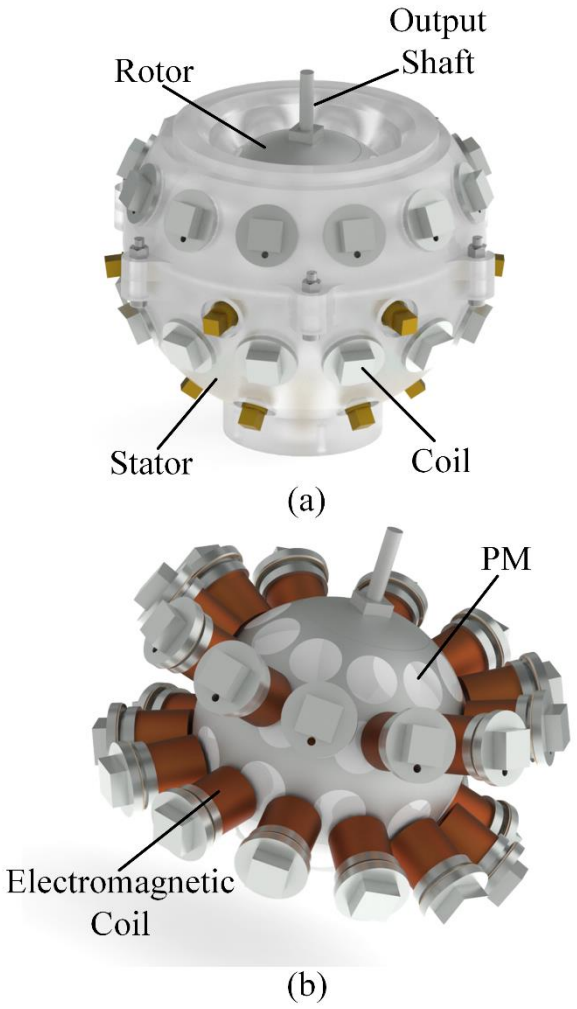

Figure 1. PMSA Structure.

2.2 PMSA drive model

In order to describe the position of the stator and the rotor, the paper defines two sets of the coordinate system of stator *xyz* and rotor *dpq*. The stator frame uses geodetic coordinates. At the initial position, the stator coordinate system coincides with the rotor coordinate system. Euler angles α, β and γ are used to express the orientation of the rotor.

For PMSA, a dynamic model based on a rigid body or rigid system can be adopted. It can be derived using the Lagrange equation as follows:

$$\boldsymbol{M}(\boldsymbol{q})\ddot{\boldsymbol{q}}+\boldsymbol{C}(\boldsymbol{q},\dot{\boldsymbol{q}})\dot{\boldsymbol{q}}+\boldsymbol{F}=\boldsymbol{\tau} \tag{1}$$

where $\boldsymbol{q}=\begin{bmatrix}\alpha & \beta & \gamma\end{bmatrix}^T$, $\dot{\boldsymbol{q}}=\begin{bmatrix}\dot{\alpha} & \dot{\beta} & \dot{\gamma}\end{bmatrix}^T$, and $\ddot{\boldsymbol{q}}=\begin{bmatrix}\ddot{\alpha} & \ddot{\beta} & \ddot{\gamma}\end{bmatrix}^T$ are the angular position, angular velocity, and angular acceleration of the rotor, respectively; $\boldsymbol{M}(\boldsymbol{q})$ is the inertial matrix; $\boldsymbol{C}(\boldsymbol{q},\dot{\boldsymbol{q}})$ is the centripetal and Coriolis matrix; $\boldsymbol{F}$ is the friction disturbance; and $\boldsymbol{\tau}\in\boldsymbol{R}^3$ is the output control torque.

For the PMSA dynamic model defined in (1), there are the following two important properties:

Property 1 The inertia matrix $\boldsymbol{M}(\boldsymbol{q})$ is symmetric, bounded and positive-definite.

Property 2 The matrix $\boldsymbol{M}(\boldsymbol{q})$- $2\boldsymbol{C}(\boldsymbol{q},\dot{\boldsymbol{q}})$ is skew-symmetric. For any nonzero vector $\boldsymbol{x} \in \boldsymbol{R}^3$, there exists $\boldsymbol{x}^T\left(\dot{\boldsymbol{M}}(\boldsymbol{q})-2\boldsymbol{C}(\boldsymbol{q},\dot{\boldsymbol{q}})\right)\boldsymbol{x}=0$.

PMs on the PMSA rotor body and the hollow coils in the stator spherical shell are symmetrically distributed in space, and because the stator coils do not contain an iron core, there is no saturation effect. Therefore, the electromagnetic torque generated by the energized coils and PMs can be calculated by the principle of superposition [17-19]. When the current supplied to the stator coil is 1A, the electromagnetic torque variation between one stator coil and one PM pole is shown in Figure 2. The discrete value of the angle-torque obtained by the finite-element method (FEM) can be used to obtain the angle-torque characteristic curve by data fitting, which is expressed by nonlinear function $f(\theta)$.

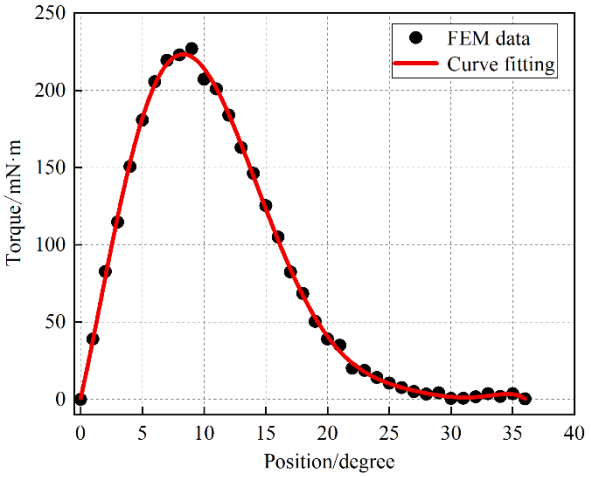

Figure 2. Angle-torque characteristic curve.

Using the principle of superposition, the torque generated by multiple different stator coils and PMs can be expressed as:

$$\boldsymbol{\tau}_{ij} = f(\theta_{ij})\frac{\boldsymbol{S}_{ri}\times\boldsymbol{S}_{rj}}{\left|\boldsymbol{S}_{ri}\times\boldsymbol{S}_{rj}\right|}I_i \tag{2}$$

where $\boldsymbol{S}_{ri}$ and $\boldsymbol{S}_{rj}$ are the PMs position vectors embedded in the rotor and the coils in the stators, respectively; I_i is the current input through the coil; θ_{ij} is a deflection angle; and $f(\theta_{ij})$ is the characteristic function. According to (2), the whole torque model can be expressed as:

$$\boldsymbol{\tau} = \sum_{i=1}^{40}\sum_{j=1}^{24} f(\theta_{ij})\frac{\boldsymbol{S}_{ri}\times\boldsymbol{S}_{rj}}{\left|\boldsymbol{S}_{ri}\times\boldsymbol{S}_{rj}\right|}I_i = \boldsymbol{A}\boldsymbol{I} \tag{3}$$

where $\boldsymbol{A}$ is the torque characteristic matrix, and $\boldsymbol{I}$ is the current matrix flowing through the 24 coils.

According to (3), the current vector calculation method required to generate the torque is selected as: $\boldsymbol{I} = \boldsymbol{A}^T\left(\boldsymbol{A}\boldsymbol{A}^T\right)^{-1}\boldsymbol{\tau}$. It can be seen that the current rising speed will have a direct impact on the magnitude of the generated torque, which will then affect the dynamic effect of the motor during operation. It is very important to choose a suitable current control algorithm for the PMSA control.

3 PID CURRENT CONTROLLER DESIGN

The topological structure of the main circuit of the current controller is shown in Figure 3. The main circuit consists of a single-phase H-bridge, a power transistor connected in series with it and a sampling resistor (R1). The H-bridge is composed of two P-MOSFETs (VT1, VT2) and two N-MOSFETs (VT3, VT4). The single-phase H-bridge circuit controls the direction of the current flowing through the stator coil, and the power transistor realizes the function of a constant current.

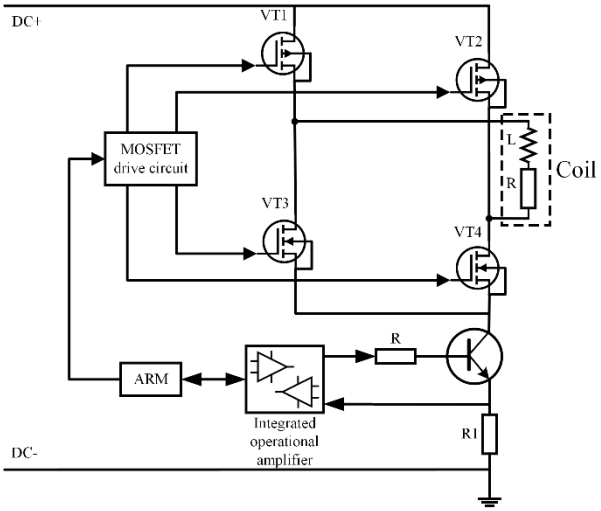

Figure 3. Main circuit topology diagram.

The current controller uses the base voltage of the transistor to control the current flowing through the collector, and the stator coil load is connected to the collector. For the base voltage to reach the desired value faster, the PID control algorithm is embedded in the main controller. This achieves the purpose of controlling the stator coil current. When the current setting value changes greatly, the dynamic response of the traditional PID control algorithm is poor, which causes the current flowing through the stator coil not to reach the expected value in time, which will affect the PMSA output torque and the motion control effect.

Ignoring the impact of the mutual inductance of the motor stator coils, the simplified stator coil voltage equation is expressed as:

$$u(t) = Ri(t) + L\frac{di(t)}{dt} \tag{4}$$

where R is the stator coil resistance and L is the stator coil self-inductance.

Using equation (4) for the Laplace transform, the stator coil transfer function is obtained as:

$$H_C(s)=\frac{1}{Ls+R} \tag{5}$$

where s is the Laplace operator. In the process of the current change, it is believed that the resistance value and the inductance value of the stator coil are basically unchanged.

3.1 Traditional PID current controller

The time domain function of the traditional PID control is:

$$u(t)=k_p\left[e(t)+\frac{1}{T_i}\int_0^t e(t)\,dt+T_d\frac{de(t)}{de}\right] \tag{6}$$

where k_p is the proportional coefficient; $e(t)$ is the current error; T_i is the integration time constant; and T_d is the differential time constant.

Equation (6) is the PID controller in a continuous time domain. But for the actual engineering application needs, it is necessary to discretize the integral and differential term, and use the form of summation and increment instead of the integral and differential form to transform it into:

$$u_k=k_p e_k+k_i\sum_{j=0}^{k}e_j+k_d\left(e_k-e_{k-1}\right) \tag{7}$$

When the control system needs to control the increment of the controlled quantity, it can adopt the incremental PID control:

$$u_k=u_{k-1}+\Delta u_k \tag{8}$$

where

$$\Delta u_k=k_p\left(e_k-e_{k-1}\right)+k_i e_k+k_d\left(e_k-2e_{k-1}+e_{k-2}\right).$$

When the sampling period is small enough, the discrete control has the same effect as the continuous control.

In the PMSA hardware drive system, the current controller outputs the voltage to the base of the power transistor to control the stator coil current. Limited by the factors, such as the drive voltage source and hardware, input voltage u_s of the controlled object will be less than output voltage u of the PID controller. The relationship between the two is as follows:

$$u_s=\begin{cases}U_{max}sgn(u) & |u|\geq U_{\max}\\ u & |u|\leq U_{\max}\end{cases} \tag{9}$$

where U_{max} is the maximum allowable amplitude of the control signal; and $sgn(x)$ is the sign function.

The structure of the PID controller with the output limitation is shown in Figure 4.

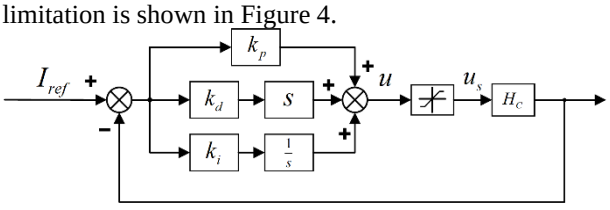

Figure 4. PID controller structure with the output limitation.

3.2 Design of the proposed anti-saturation PID current controller

When PMSA performs a motion control, the reference current value calculated by the torque is in a fast and continuous dynamic change process. The current value calculated each time is a step input, and the time for each calculation is extremely short. The integral saturation makes the current change slowly. The stator coil current does not reach a stable state, and the system will give a reference value for controlling the current at the next moment. This may cause the actual motor output shaft movement to fail in reaching the desired position in time due to the slow current change speed.

In order to suppress the impact of the integral saturation on the current control system, it is necessary to modify the controller integral link. The idea of the anti-integral-saturation PID controller is to add anti-saturation gain k_a to the controller. When calculating u_k, first judge whether control quantity u_{k-1} at the previous moment exceeds the limit range. If $u_{k-1}>U_{max}$, only the negative deviation will be accumulated; if $u_{k-1}<U_{max}$, only the positive deviation will be accumulated. The structure diagram of the anti-saturation PID controller is shown in Figure 5.

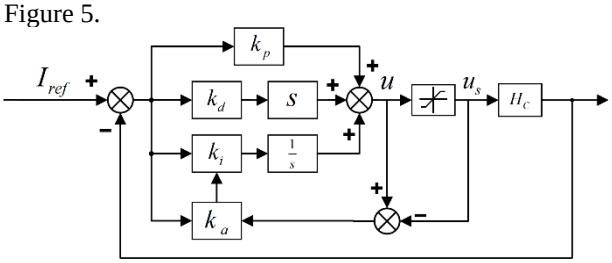

Figure 5. Anti-saturation PID controller structure.

An addition of the anti-saturation gain reduces the negative impact on the control system due to the untimely current change. The response speed of the stator coil current can be improved when the system is started or the set value is greatly changed, so that the actual output value can better follow the change in the given reference value, and a better control effect can be achieved.

4 EXPERIMENT

4.1 Introduction of the proposed current controller

In order to verify the effectiveness of the proposed anti-saturation PID current controller, a hardware experimental platform, including an ARM digital signal controller, host computer, coil, serial port and oscilloscope, is built. The experimental setup is shown in Figure 6. First, the experiment is carried out on a single current controller.

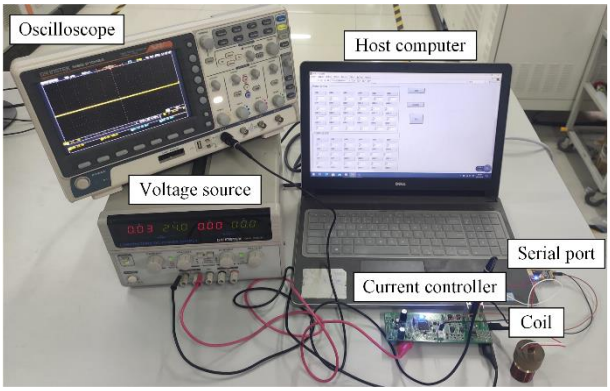

Figure 6. Current controller.

In the experimental setup, the voltage source supplies the power to the current controller, which is connected to the stator coil. The host computer sends the reference current value to the current controller through a serial port. The master controller executes the proposed control algorithm. The flow chart of the anti-integral saturation PID control algorithm in the current controller is shown in Figure 7.

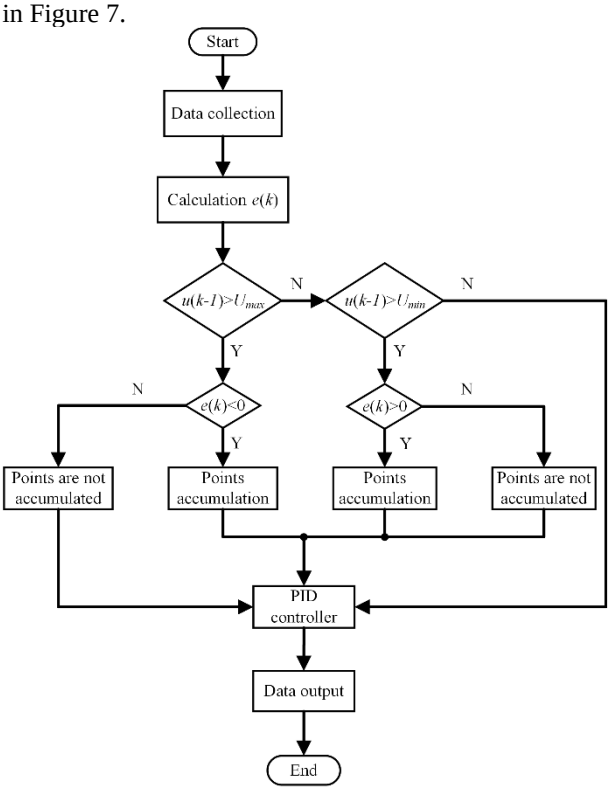

Figure 7. Anti-saturation PID algorithm flow chart.

4.2 Current control experiment and analysis

Firstly, the current rise time of a single stator coil is tested. The traditional PID controller, the incremental PID controller and the anti-saturation PID controller proposed in the paper are used for a comparative experiment. The experimental stator-coil parameters are measured by an LCR tester with the coil resistance of 6.99Ω and coil inductance of 7.75mH. The output voltage of the DC controller is set at 24V, the reference current value is set at 2A through the upper computer, an oscilloscope is uesd to measure the rising time of the current at both ends of the stator coil, and parameters of the three current controllers are set as shown in Table 2. Using the three controllers, the rising time of the current at both ends of the stator coil is shown in Figure 8.

Table 2. Current controller parameter setting

Algorithm	k_p	k_i	k_d	k_a
PID	0.52	0.02	0.10	—
Incremental PID	0.52	0.02	0.10	—
Anti-saturation PID	0.52	0.02	0.10	1.0

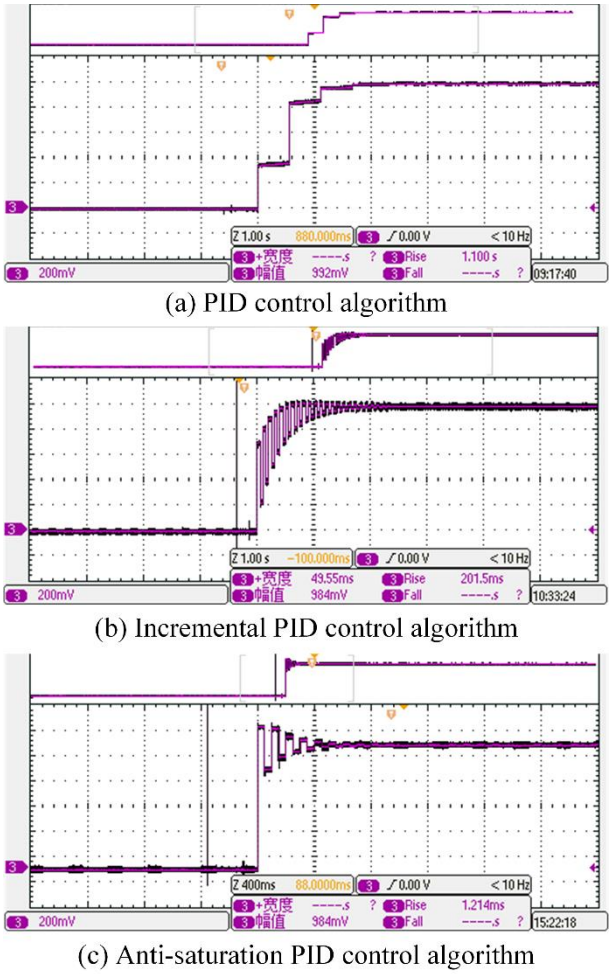

Figure 8. Stator coil current waveforms.

In the above three controllers, the current is set at the same value. When using the traditional PID controller, the current rise speed is too slow. When using the anti-integral saturation PID controller, the current rise time is significantly reduced. When using the proposed anti-saturation PID controller, besides the significantly reduced rise time, there are also fewer current jitter phases and no obvious current step-up phase, and a steady state is reached faster.

In our comparative experiment, different current values are set by the host computer in the above three controllers. Thus obtained current rise times are shown in Table 3.

Table 3. Comparison of the current rise times

Set value	Current rise time		
	PID	Incremental PID	Anti-saturation PID
0.5A	1.2s	0.6s	0.3s
1.0A	1.3s	0.8s	0.4s
1.5A	1.5s	0.9s	0.5s
2.0A	1.6s	1.2s	0.6s
2.5A	1.7s	1.4s	0.7s
3.0A	2.0s	1.7s	0.9s

As seen from Table 3, when different currents are used, using the proposed controller greatly reduces the current response time of the stator coil, compared to the PID controller and the incremental PID controller. Using the proposed anti-saturation PID controller reduces the current rise time by about 50%.

4.3 Control experiment

To verify the impact of the proposed anti-saturation PID current controller on the PMSA control system, a PMSA motion experiment is carried out on an experimental setup composed of PMSA, host computer, current driver and position sensor. The experimental setup is shown in Figure 9.

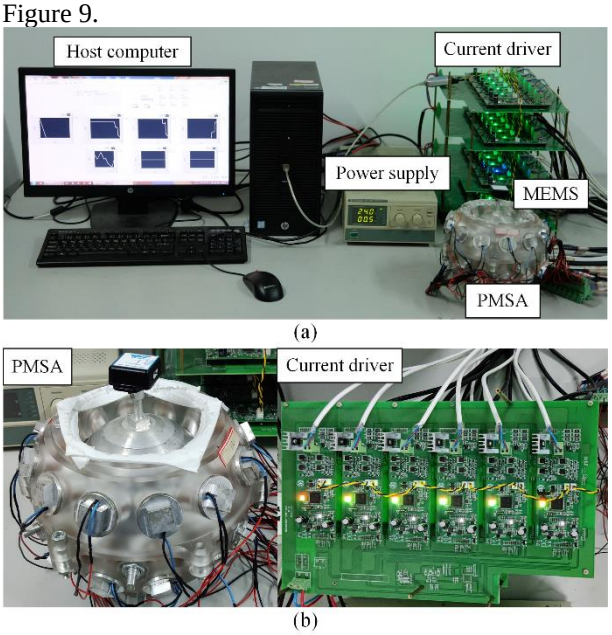

Figure 9. Experimental setup.

In the experimental setup, the current driver contains 24 independent current controllers which provide the current to 24 stator coils. The position information is obtained by a position sensor mounted on the output shaft. The host computer obtains the position information of the PMSA output shaft by MEMS and the output torque by the control algorithm. It then calculates the reference current value of the 24 stator coils according to the drive model given in Section 2.2. The calculated reference current value is sent to the current driver by a serial port to make the rotor move.

In order to verify the impact of the anti-saturation PID current driver on the control system, a relatively simple PD control algorithm is used in the host computer to control PMSA and make the output shaft carry out the tilt motion and spin motion. In the current driver, the traditional PID controller and proposed anti-saturation PID controller are compared. The experimental result are shown in Figure 10 and Figure 11, respectively.

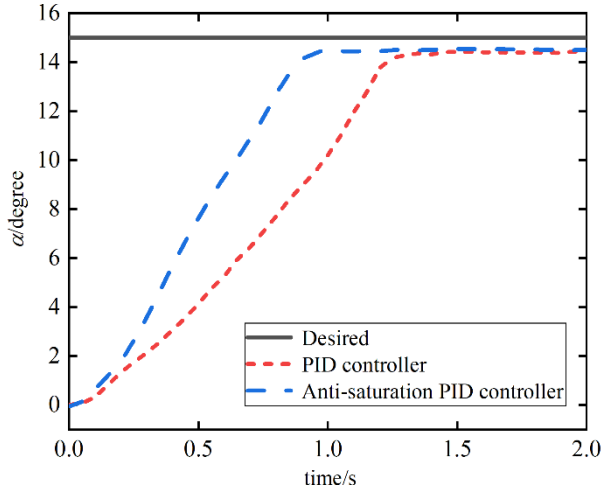

Figure 10. Tilt motion graph.

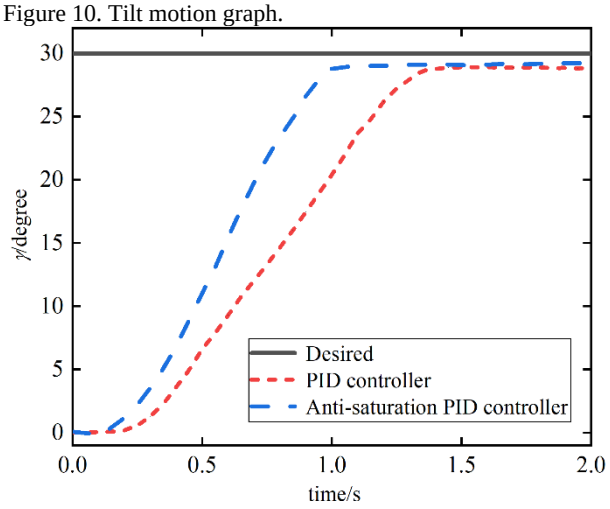

Figure 11. Spin motion graph.

As seen from the experimental results, when the host computer adopts the same control algorithm, using the proposed anti-saturation PID control algorithm in the current driver improves the response speed of the motor during operation, thus make the output shaft to reach the desired position faster. Besides the algorithm in the controller, the communication delay between the host computer and the driver and the resistive load itself also affect the current response speed. An analysis of the experimental results is shown in Table 4.

Table 4. Analysis of the experimental results

	Parameter	PID	Anti-saturation PID
Tilt motion	Respond speed	1.2s	0.9s
	Steady state error	0.6degree	0.5degree
Spin motion	Respond speed	1.4s	1.1s
	Steady state error	1.1degree	0.9degree

Table 4 shows that when using the proposed anti-saturation PID control algorithm in the current driver, both the response time and the steady-state error are smaller than when using the traditional PID control. Using the method proposed in the paper improves the current control. The response time reduced by about 20%, improves the control system dynamic response effect.

5 CONCLUSION

Using a traditional PID controller in the PMSA drive control system gives an integral saturation phenomenon. To avoid it, the paper proposes an anti-integral-saturation PID control method to add an anti- saturation gain to the traditional PID controller. By comparing experimental results obtained with the traditional, incremental and the proposed PID controller, it is shown that the latter outperforms the former two in forms of the dynamic current response speed in the level of 50%. The method is simple in structure and easy to design and implement, which solves the problem of a too slow current response of the stator coil current at running actuator. Moreover, experimental results show that the PMSA dynamic performance is improved by 20%, thus providing the grounds for PMSA engineering applications.

ACKNOWLEDGEMENT

The work was financially supported by the Key Project of the China National Natural Science Foundation (No. 51637001).

REFERENCES

[1] Day, C.P. "Robotics in Industry—Their Role in Intelligent Manufacturing", in: Engineering, 2018, vol. 4, no. 4, pp. 27-39, ISSN 0029-8018

[2] Li, L.Q., Fang, Y.F., Wang, L. "Design of a family of multi-DOF drive systems for fewer limb parallel mechanism", in: Mechanism and Machine Theory, 2019, vol. 148, pp. 1-16, ISSN 0094-114X

[3] Li, Z., Lun, Q., Xing, D., Gao, P. "Analysis and Implementation of a 3-DOF Deflection-Type PM Motor", in: IEEE Transactions on Magnetics, 2015, vol. 51, no. 11, pp. 1-4, ISSN 0018-9464

[4] Kim, K., Ahn, D., Gweon, D. "Optimal design of a 1-rotational DOF flexure joint for a 3-DOF H-type stage", in: Mechatronics, 2012, vol. 22, no. 1, pp. 24-32, ISSN 0957-4158

[5] Guo, X.W., Wang, Q.J., Li, G.L. "Research and development of Multi-Degree-of-Freedom permanent magnet spherical motor's control strategy", in: Weite Dianji/Small & Special Electrical Machines, 2011, vol. 39, no. 2, pp. 72-76, ISSN 1004-7018

[6] Li, X.R., Liu, J.M., Chen, W.H., Bai, S.P. "Integrated design, modeling and analysis of a novel spherical motion generator driven by electromagnetic principle", in: Robotics and Autonomous Systems, 2018, vol. 106, no. 1, pp. 69-81, ISSN 0921-8890

[7] Son, H., Lee, K.M. "Control system design and input shape for orientation of spherical wheel motor", in Control Engineering Practice, 2014, vol. 24, no. 3, pp. 120-128, ISSN 0967-0661

[8] Huang, J.G., Wang, J., Fang, H. "An anti-windup self-tuning fuzzy PID controller for speed control of brushless DC motor", in: Automatika, 2017, vol. 58, no. 3, pp. 321-335, ISSN 0005-1144

[9] Li, X.L., Park, J.G., Shin, H.B. "Comparison and Evaluation of Anti-Windup PI Controllers", in: Journal of Power Electronics, 2011, vol. 11, no. 1, pp. 45-50, ISSN 1598-2092

[10] Liu, Y.S., Zhu, T.Y., Wu, S.L., Li, S.L., Wu, B.Y., Huang, Z.F. "Model Predictive Current Control of Dual-Permanent-Magnet Vernier Motor based on Anti-Windup Controller", in: IOP Conference Series: Earth and Environmental Science, 2020, vol. 619, no. 1, pp. 12037-12046, ISSN 1755-1307

[11] Yu, Y.J., Chai, F., Gao, H.W., Chen, S.K. "Design of PMSM system based on anti-windup controller", in: Diangong Jishu Xuebao/Transactions of China Electrotechnical Society, 2009, vol. 24, no. 4, pp. 66-70, ISSN 1000-6753

[12] Li, X.L., Park, J.G., Shin, H.B. "Comparison and evaluation of anti-windup PI controllers", in: Journal of Power Electronics, 2011, vol. 11, no. 1, pp. 45-50, ISSN 1598-2092

[13] Shin, H.B., Park, J.G. "Anti-Windup PID controller with integral state predictor for variable-speed motor drives", in: IEEE Transactions on Industrial Electronics, 2011, vol.59, no. 3, pp. 1509-1516, ISSN 0278-0046

[14] Kawai, F., Vinther, K., Andersen, P., Bendtsen, J.D. "Anti-windup disturbance feedback control: Practical design with robustness", in: Journal of Process Control, 2018, vol.69, no. 5, pp. 339-350, ISSN 0019-0578

[15] Lu, Y., Hong, Y., Hu, C.G., Rong, Y.P. "Position detection method for permanent magnet spherical motors based on MEMS", in: Dianji yu Kongzhi Xuebao/Electric Machines and Control, 2019, vol. 23, no. 8, pp. 87-95, ISSN 1007-449X

[16] Wen, Y., Li, G.L., Wang, Q.J., Guo, X.W. "Robust adaptive sliding-mode control for permanent magnet spherical actuator with uncertainty using dynamic surface approach", in: Journal of Electrical Engineering and Technology, 2019, vol. 14, no. 6, pp. 2341-2353, ISSN 1975-0102

[17] Guo, X.W., Li, S., Wang, Q.J., Zhou, R., Wen Yan. "Analysis of torque characteristics and electrifying strategy of permanent magnet spherical motor based on triangular combination coils", in: Diangong Jishu Xuebao/Transactions of China Electrotechnical Society, 2019, vol. 34, no. 8, pp. 1607-1615, ISSN 1000-6753

[18] Wen, Y., Li, G.L., Wang, Q.J., Cao, W.P. "Modeling and analysis of permanent magnet spherical motors by a multi-task gaussian process method and finite element method for output torque", in: IEEE Transactions on Industrial Electronics, 2020, vol. 68, no. 9, pp. 8540-8549, ISSN 0278-0046

[19] Wen, Y., Li, G.L., Tang, R.Y., Li, H.L. "Investigation on the measurement method for output torque of a spherical motor", in: Applied Sciences, 2020, vol. 10, no. 7, pp. 1-16, ISSN 0170-4214

Rui Zhang graduated from the Anhui Agricultural University, China, in 2015. He is currently working towards his M.Sc. degree at the School of Electrical Engineering and Automation of Anhui University, China. His research interests include hardware drive design and optimization and control strategies of permanent magnet spherical actuator.

Guoli Li received her Ph.D. degree in electrical engineering from ASIPP, Hefei, China, in 2008. Currently, she is a professor at the School of Electrical Engineering and Automation of Anhui University, China. Her research interests are in electrical & electronic engineering and intelligent optimization techniques.

Qunjing Wang received his Ph.D. degree from the University of Science and Technology of China, Hefei, China, in 2001. Currently, he is a professor at the School of Electrical Engineering and Automation at Anhui University, China. His research interests are in electrical machines, motor drives and novel electric drive systems.

Xiuqin Wang received her Ph.D. degree in electrical engineering from the Anhui University, China, in 2019. Currently, she is a lecturer at the School of Electrical Engineering and Automation at the Anhui University, China. Her research interest is in the research and development of power quality devices.

Yan Wen received her Ph.D. degree in electrical engineering from the Anhui University, China, in 2020. Currently, she is a lecturer at the School of Internet at Anhui University, China. Her research interests include the novel spherical actuator and its control & orientation measurement, complex system modelling and analysis.